# Max-Planck-Institut
## für Mathematik
## in den Naturwissenschaften
## Leipzig


**Numerical Method for Elliptic Multiscale Problems**

by


*Isabelle Greff, and Wolfgang Hackbusch*



Preprint no.: 138 2006


# Numerical Method for Elliptic Multiscale Problems

Isabelle Greff, Wolfgang Hackbusch

**Abstract**

In this paper we are interested in the coarse-mesh approximations of a class of second order elliptic operators with rough or rapidly oscillatory coefficients. We intend to provide a smoother elliptic operator which on a coarse mesh behaves like the original operator. Note that there is no requirement on smoothness or periodicity of the coefficients. To simplify the theory and the numerical implementations, we restrict ourselves to the one-dimensional case.

## 1 Introduction

A large class of multiscale problems are described by partial differential equations with highly oscillatory coefficients. Such coefficients represent the properties of a composite material or the heterogeneity of the medium in the computation of flow in porous media problems. The computation of an accurate discrete solution of such problems requires a very fine discretisation associated with a fine grid $\mathcal{T}_h$. For such a fine resolution, the storage and computation costs are very high. From an engineer's perspective, we are interested in the average behaviour of the elliptic oscillatory operator on a coarse scale taking into account the small scale features without fully resolving them. Therefore we focus on the computation of the discrete solution on a coarse mesh taking into account as much information as possible about the oscillatory coefficients.
As a model problem, let us consider the elliptic boundary value problem on $\Omega$, a bounded Lipschitz domain in $\mathbb{R}^d$,

$$\begin{cases} Lu = f & \text{in } \Omega, \\ u = 0 & \text{on } \partial\Omega, \end{cases} \tag{1}$$

with the right-hand side $f$ in $L^2(\Omega)$. As an example, let

$$L = -\sum_{i,j=1}^{d} \frac{\partial}{\partial_j} \alpha_{ij} \frac{\partial}{\partial_i},$$

whose coefficients may contain a small-scale parameter, *e.g.*, $\alpha_{ij} \in L^\infty(\Omega)$ is an oscillatory or jumping coefficient. We require certain real numbers $\underline{\lambda}, \overline{\lambda} > 0$ such that the matrix function $\alpha(x) = (\alpha_{ij})_{i,j=1,\dots,d}$ satisfies $0 < \underline{\lambda} \leq \lambda(\alpha(x)) \leq \overline{\lambda}$ for all eigenvalues $\lambda(\alpha(x))$ of $\alpha(x)$ and almost all $x \in \Omega$.

Our goal is to construct an elliptic operator $A$ with slowly varying coefficients which behaves similarly to the operator $L$ on a coarse grid. We are looking for an operator $A = -\operatorname{div}(a \cdot \nabla)$ with $a$ smoother than $\alpha$. To build $A$, we will consider the prolongation and restriction operators issued from the multi-grid method framework, and combine them with $L$. Among various approaches, let us mention types of methods like Heterogeneous Multiscales Method [15] and Multiresolution Methods [5]. A different numerical method to solve such a problem is the so-called generalised finite element method introduced in 1D by Babuška-Osborn [2], and generalised to 2D by Hou and Wu [11, 12]. The principle behind this method is to construct modified basis functions adapted to the oscillations of the differential operator. Another possibility is the variational multiscale approach introduced by Hughes [13, 14] and Brezzi [6], where the trial and test spaces are split into two sub-spaces representing the fine and the coarse scales respectively. Arbogast developed a mixed variant of this method in [1].

To simplify the theory, we restrict ourselves to the one-dimensional case. Let $\Omega = (0, 1)$ and $V = H_0^1(\Omega)$. Let $L : V \to V'$ be the elliptic operator $L = -\frac{d}{dx}(\alpha(x)\frac{d}{dx})$ with an oscillatory coefficient $\alpha > 0$, $\alpha \in L^\infty(\Omega)$. Let us consider the following problem

$$\begin{cases} L\,u = f & \text{in } \Omega \\ u(0) = u(1) = 0\,. \end{cases} \tag{2}$$

The computation of an accurate discrete solution of problem (2) with a strongly oscillatory coefficient $\alpha$ leads to a very fine discretisation related to a fine grid $\mathcal{T}_h$, in particular high requirements of storage and computation operations. On the other hand, we are more interested in the average behaviour of the solution on a coarse level which captures the smooth part of the solution. Then, we consider a regular coarse grid $\mathcal{T}_H$ of $\Omega$, describing the macroscopic level. The step size is $H = 1/(m+1)$. The nodes are $0 = x_0^H < \ldots < x_j^H < \ldots < x_{m+1}^H = 1$. We define the standard linear FE-space $V_H$ related to $\mathcal{T}_H$ vanishing at the boundary nodes by $V_H = \operatorname{span}\{b_1^H, \ldots, b_m^H\}$ of dimension $\dim V_H = m$.

Let $\mathcal{P}_H$ be some prolongation from the macroscopic level to the continuous level and $\mathcal{R}_H$ a restriction operator associated to $\mathcal{P}_H$. Using the Green function of the operator $L$, it is possible to consider the following problem:

**Problem 1.1** *Let $\mathcal{L}_H \in \mathbb{R}^{m\times m}$ be defined by*

$$\mathcal{L}_H := \left(\mathcal{R}_H L^{-1} \mathcal{P}_H\right)^{-1}. \tag{3}$$

*Can $\mathcal{L}_H$ be interpreted as an approximation $A_H$ of some local differential operator $A$ with the step size $H$?*

Since the Green function is not always explicitely given, in a practical point of view, we could consider a very small step size $h$ and the discretisation of the operator $L$ on a fine grid $\mathcal{T}_h$. Let us introduce a regular fine grid $\mathcal{T}_h$ which resolves the small details of the elliptic operator $L$. The grid $\mathcal{T}_h$ is finer as $\mathcal{T}_H$, the parameter $h$ is smaller than $H$. The nodes of the grid are $0 = x_0^h < \ldots < x_j^h < \ldots < x_{n+1}^h = 1$ with $n \gg m$ and the step size $h = 1/(n+1)$. Let $V_h$ be the standard $P^1$-Lagrange FE space vanishing at the boundary nodes, with the nodal basis $\{b_1^h, \ldots, b_n^h\}$ and the dimension $\dim V_h = n$. The grid $\mathcal{T}_H$ is nested in $\mathcal{T}_h$ in the sense that $V_H \subset V_h$. We define an isomorphism $P_h$ by

$$P_h : \mathbb{R}^n \to V_h \subset V$$
$$v = (v_1, \ldots, v_n) \longmapsto P_h\, v = \sum_{i=1}^{n} v_i\, b_i^h$$

and its adjoint $R_h = P_h^* \in L(V', \mathbb{R}^n)$. The mass matrices are $M_h \in \mathbb{R}^{n\times n}$ and $M_H \in \mathbb{R}^{m\times m}$ given by $M_h = R_h\, P_h$ and $M_H = R_H\, P_H$ (where $P_H$ is defined the same way as $P_h$ on the coarse grid). The FE stiffness matrix $L_h$ is given by $L_h = R_h\, L\, P_h$. Let $u \in V$ be the solution of the variational problem associated with (2):

$$\int_\Omega \alpha(x) \frac{d\,u}{dx} \frac{d\,v}{dx}\, dx = \int_\Omega f\, v$$

and $u_h$ be its Ritz discretisation in $V_h$. The weakest form of the finite element convergence is described by

$$\|u - u_h\|_{L^2(\Omega)} \le \varepsilon(h)\, \|f\|_{L^2(\Omega)} \quad \text{for all } u = L^{-1} f,\ f \in L^2(\Omega)\,, \tag{4}$$

where $\|u - u_h\|_{L^2(\Omega)}$ is the FE-error and $\varepsilon(h) \to 0$ as $h \to 0$ (see [3]).

The inclusion $V_H \subset V_h$ ensures that the following mappings are well defined: the prolongation operator $P_{h\leftarrow H}$ from the coarse grid $\mathcal{T}_H$ to the fine grid $\mathcal{T}_h$ given by

$$P_{h\leftarrow H} = (P_h^{-1}\, P_H) : \mathbb{R}^m \longrightarrow \mathbb{R}^n$$

and the restriction operator $R_{H\leftarrow h} = \left(P_{h\leftarrow H}\right)^*$ from the fine grid $\mathcal{T}_h$ to the coarse grid $\mathcal{T}_H$. Let us define the normalised prolongation and restriction (also defined in [9]):

$$\tilde{P}_{h\leftarrow H} : \mathbb{R}^m \to \mathbb{R}^n \ \text{ by } \ \tilde{P}_{h\leftarrow H} = M_h\, P_{h\leftarrow H}\, M_H^{-1} \ \text{ and } \ \tilde{R}_{H\leftarrow h} = \left(\tilde{P}_{h\leftarrow H}\right)^*.$$

With help of $\mathcal{H}$-arithmetic (see [8]) the computation of the discrete operator $L_h^{-1}$ on the fine mesh is possible. Therefore the following matrix $\mathcal{L}_{H,h}$ is available

$$\mathcal{L}_{H,h} := \left(\tilde{R}_{H\leftarrow h} L_h^{-1} \tilde{P}_{h\leftarrow H}\right)^{-1}.$$

We can now reconsider Problem 1.1 with the operator $\mathcal{L}_{H,h}$ approximating the continuous operator $\mathcal{L}_H$ on the coarse mesh $\mathcal{T}_H$. We get the following derived problem:

**Problem 1.2** *We are looking for an elliptic operator $A \in L(V, V')$ such that its discretisation $A_H$ on the coarse grid satisfies:*

$$A_H \approx \mathcal{L}_{H,h} \quad \text{for all } h \text{ small enough.} \tag{5}$$

One way of finding the elliptic operator $A$ is to consider an "inverse" Taylor expansion of the matrix $\mathcal{L}_{H,h}$. Considering the matrix $\mathcal{L}_{H,h}$, it is possible to compute numerically some coefficients $\beta_{i,h}$ depending on $h$, converging towards $\beta_i$ when $h \to 0$, such that

$$A \approx \sum_{i=0}^{n} \beta_i(x) \frac{d^i}{dx^i} \tag{6}$$

holds, where $\frac{d^i}{dx^i}$ denotes the $i$th-derivative. We expect the coefficients $\beta_i$ to vanish for $i > 2$.

On the other hand, we consider the special case of $T$-periodic coefficients $\alpha$. Let $L_0 = -\alpha_0 \frac{d^2}{dx^2}$ be the homogenised operator associated with $L$ (see [4]) where

$$\alpha_0 \;=\; \frac{1}{M(\frac{1}{\alpha})} \quad \text{and} \quad M\Big(\frac{1}{\alpha}\Big) = \frac{1}{T}\int_0^T \frac{dx}{\alpha(x)}. \tag{7}$$

It is well known that the exact solution $u = L^{-1}f$ of (2) is approximated by the homogenised one $u_0 = L_0^{-1}f$ with a precision depending on the period $T$. Then, the homogenisation theory should provide a good operator, solution of problem (5). However, our goal is more general and we intend to find an operator $A$ satisfying (5), without any restriction on the periodicity of the coefficient $\alpha$. For this purpose let us consider the elliptic operator $A$, defined by $A = -\frac{d}{dx}\Big(a\frac{d}{dx}\Big)$, where the coefficient $a$ is defined on each segment $[x_j^H, x_{j+1}^H]$ by

$$a_{|[x_j^H, x_{j+1}^H]} = \frac{1}{\theta_j} \quad \text{where} \quad \theta_j = \frac{1}{x_{j+1}^H - x_j^H}\int_{x_j^H}^{x_{j+1}^H} \frac{ds}{\alpha(s)}\,. \tag{8}$$

Particularly for a $T$-periodic coefficient $\alpha$, with $H > T$ and $H$ and $T$ proportional, the choice of (8) gives $a = \frac{1}{M(\frac{1}{\alpha})} = \alpha_0$, *i.e.* $a$ is the homogenised coefficient associated with $\alpha$.

Let $\|\cdot\|_2$ be the Euclidean norm. According to [10], we introduce the norm $\|\!|\cdot|\!\|$ defined for a matrix $X \in \mathbb{R}^{m\times m}$ by

$$|\!|\!|X^{-1}|\!|\!| := \|P_H\, X^{-1} R_H\|_{L^2(\Omega)\leftarrow L^2(\Omega)} = \|M_H^{1/2} X^{-1} M_H^{1/2}\|_2\,. \tag{9}$$

We are going to prove that the discrete operator $\mathcal{L}_{H,h}$ is behaving as a discretisation of an elliptic operator, namely $A$. For this purpose the paper is organised as follows. We begin to describe the relations between the Green functions of $L$ and $L_0$ (*i.e.* the restriction of the operator $A$ to the periodic case). In Section 3, we prove the main theorem in the case of a positive periodic coefficient $\alpha$. It gives the accuracy of the approximation $\mathcal{L}_{H,h}$ to the discrete homogenised solution operator $A$. Finally in Section 4, some numerical results for different types of coefficient $\alpha$ (periodic or not) demonstrate the method.

# 2 Green's function

Let us consider the case of a $T$-periodic coefficient $\alpha$. The Green function $G$, associated with the operator $L$, is given explicitly for homogeneous boundary conditions by

$$G(x,t) = -H(x-t)\int_t^x \frac{ds}{\alpha(s)} + \frac{1}{M(\frac{1}{\alpha})}\Big(\int_t^1 \frac{ds}{\alpha(s)}\Big)\Big(\int_0^x \frac{ds}{\alpha(s)}\Big), \quad x \in [0,1],\, t \in [0,1],$$

where $H(\cdot)$ is the Heaviside function. From this formula we deduce the following lemma.

**Lemma 2.1** *The Green function $G$ of the elliptic operator $L$ can be decomposed as $G(x,t) = G_0(x,t) + R_T(x,t)$, where $G_0$ is the Green function associated with the homogenised operator $L_0$*

$$G_0(x,t) = -M\Big(\frac{1}{\alpha}\Big)\Big((x-t)\,H(x-t) - x\,(1-t)\Big), \quad x \in [0,1]\,,\; t \in [0,1]\,,$$

*and $R_T$ is the remaining part given by*

$$R_T(x,t) = -H(x-t)\big(D(T,t_0)+D(x_0,0)\big)+\frac{1}{M(\frac{1}{\alpha})}\,D(x_0,0)\,D(T,t_0) \\ +x\,D(T,t_0)+(1-t)\,D(x_0,0)\,, \quad x\in[0,1]\,,\ t\in[0,1]\,,$$

*where $x_0$, $t_0 \in [0,T[$ such that there exist $k$, $l \in \mathbb{N}$ satisfying $x = x_0 + kT$, $t = t_0 + lT$, and $D(x,y) = \int_y^x \frac{ds}{\alpha(s)} - M(\frac{1}{\alpha})(x-y)$.*

# 3 Theoretical result

Let $L_{0,H}$ be the discretisation of $L_0$ in the space $V_H$. Let $\varepsilon_0(H)$ be the bound of its FE-discretisation error defined in the same way as (4). In this section, we assume that the step size $H$ is larger than $T$, and $T$ and $H$ are proportional, which gives $A = L_0$. We compare the discrete operators $\tilde{R}_{H\leftarrow h}\,L_h^{-1}\tilde{P}_{h\leftarrow H}$ and $L_{0,H}^{-1}$ defined on the coarse level. Let $B_h$ be the Galerkin discretisation of the inverse of $L$, defined by $B_h = R_h\,L^{-1}\,P_h$. Each element of the matrix $B_h$ is given as a function of the Green function $G$,

$$\big(B_h\big)_{i,j} = \int_\Omega b_i^h(x)\int_\Omega G(x,t)\,b_j^h(t)\,dt\,dx \quad \text{for all } 1\le i,j\le n\,. \tag{10}$$

In the same way, we define $B_{0,h}$ and $B_{0,H}$ to be the Galerkin discretisations of the inverse of $L_0$ respectively on the coarse and fine grids: $B_{0,H} = R_H\,L_0^{-1}\,P_H$ and $B_{0,h} = R_h\,L_0^{-1}\,P_h$. From [3], Corollary 5.3, we have the following bounds on the difference between the inverse of the stiffness matrices and the Galerkin discretisation of the inverse operators:

$$\begin{array}{c} ||L_{0,H}^{-1} - M_H^{-1}\,B_{0,H}\,M_H^{-1}||_2 \le 2\,\|M_H^{-1}\|_2\,\varepsilon_0(H)\,, \\ ||L_h^{-1} - M_h^{-1}\,B_h\,M_h^{-1}||_2 \le 2\,\|M_h^{-1}\|_2\,\varepsilon(h)\,. \end{array} \tag{11}$$

The comparison of both operators $L$ and $L_0$ is achieved through the estimation of the norm $\|\!|\tilde{R}_{H\leftarrow h}\,L_h^{-1}\tilde{P}_{h\leftarrow H} - L_{0,H}^{-1}|\!\|$ by the next theorem.

**Theorem 3.1** *The following error estimate holds*

$$|\!|\!|\tilde{R}_{H\leftarrow h}\,L_h^{-1}\tilde{P}_{h\leftarrow H} - L_{0,H}^{-1}|\!|\!| \;\le\; C\,\Big(\varepsilon(h) + T\,M\big(\frac{1}{\alpha}\big)\,(1+T) + \varepsilon_0(H)\Big), \tag{12}$$

*where $\varepsilon(h)$ is a bound on the error of the FE-discretisation of $L$ on the fine mesh $\mathcal{T}_h$, and $\varepsilon_0(H)$ is the bound on the error of the homogenised FE-discretisation of $L_0$ on the coarse mesh $\mathcal{T}_H$.*

**Proof** Let us consider the Galerkin matrices $B_{0,h}$ and $B_{0,H}$, resulting from the discretisation of $L_0^{-1}$ on both the fine and the coarse grids. We prove that

$$\tilde{R}_{H\leftarrow h}\,(M_h^{-1}B_{0,h}M_h^{-1})\tilde{P}_{h\leftarrow H} = M_H^{-1}B_{0,H}M_H^{-1}\,, \tag{13}$$

by using the definitions of $\tilde{R}_{H\leftarrow h}$ and $\tilde{P}_{h\leftarrow H}$ and the well-defined formula $R_{H\leftarrow h}\,R_h = R_H$.
In view of the decomposition $G(x,t) = G_0(x,t) + R_T(x,t)$, the matrix $B_h$ defined by (10) can be written as $B_h = B_{0,h} + B_{T,h}$, where $B_{0,h}$ is the homogenised Galerkin matrix for $L_0^{-1}$ and $B_{T,h}$ is the remainder part which will be defined in Lemma 3.1. Lemma 3.1 will also give a bound of $B_{T,h}$. Let us rewrite the term $\tilde{R}_{H\leftarrow h}\,L_h^{-1}\tilde{P}_{h\leftarrow H} - L_{0,H}^{-1}$ in the following form

$$\begin{aligned} \tilde{R}_{H\leftarrow h}\,L_h^{-1}\tilde{P}_{h\leftarrow H} - L_{0,H}^{-1} \;=\; & \tilde{R}_{H\leftarrow h}\,(L_h^{-1} - M_h^{-1}B_hM_h^{-1})\tilde{P}_{h\leftarrow H} + \tilde{R}_{H\leftarrow h}\,M_h^{-1}B_hM_h^{-1}\tilde{P}_{h\leftarrow H} \\ & -M_H^{-1}B_{0,H}M_H^{-1} + (M_H^{-1}B_{0,H}M_H^{-1} - L_{0,H}^{-1})\,. \end{aligned}$$

Using the decomposition $B_h = B_{0,h} + B_{T,h}$ and equality (13), we get

$$\begin{aligned} \tilde{R}_{H\leftarrow h}\,L_h^{-1}\tilde{P}_{h\leftarrow H} - L_{0,H}^{-1} \;=\; & \tilde{R}_{H\leftarrow h}\,(L_h^{-1} - M_h^{-1}B_hM_h^{-1})\tilde{P}_{h\leftarrow H} + \tilde{R}_{H\leftarrow h}\,M_h^{-1}B_{T,h}M_h^{-1}\tilde{P}_{h\leftarrow H} \\ & +(M_H^{-1}B_{0,H}M_H^{-1} - L_{0,H}^{-1})\,. \end{aligned}$$

We have the following estimates for the mass matrices and the prolongation operators:

$$\|M_h\|_2 \le C\,h\,, \quad \|M_h^{-1}\|_2 \le C\,h^{-1}\,, \quad \|P_{h\leftarrow H}\|_2 \le C\,\Big(\frac{H}{h}\Big)^{1/2}, \quad \|\tilde{P}_{h\leftarrow H}\|_2 \le C\,\Big(\frac{h}{H}\Big)^{1/2}. \tag{14}$$

On the other hand $\big\|B_{T,h}\big\|_2$ is bounded (see Lemma 3.1) by

$$\big\|B_{T,h}\big\|_2 \le C\,h\,T\,M\Big(\frac{1}{\alpha}\Big)\,(1+T)\,. \tag{15}$$

So from estimates (11), (14), and (15), we get the intermediate estimate

$$\|\tilde{R}_{H\leftarrow h}\,L_h^{-1}\tilde{P}_{h\leftarrow H} - L_{0,H}^{-1}\|_2 \quad \le \quad C\,\Big(\varepsilon(h) + M\Big(\frac{1}{\alpha}\Big)\,T\,(1+T) + \varepsilon_0(H)\Big)H^{-1}.$$

Due to definition (9), $\|\!|\tilde{R}_{H\leftarrow h}\,L_h^{-1}\tilde{P}_{h\leftarrow H} - L_{0,H}^{-1}|\!\| \le \|M_H\|_2\,\|\tilde{R}_{H\leftarrow h}\,L_h^{-1}\tilde{P}_{h\leftarrow H} - L_{0,H}^{-1}\|_2$ holds, which gives (12). ■

Let us evaluate the norm of the matrix $B_{T,h}$ defined for the remaining part $R_T$ on the fine grid $\mathcal{T}_h$ by $\big(B_{T,h}\big)_{i,j} = \int_\Omega b_i^h(x)\int_\Omega R_T(x,t)\,b_j^h(t)\,dt\,dx$. We get the following result.

**Lemma 3.1** *There exists a certain constant $C$, independent of $T$, $h$, and $H$ such that*

$$\|B_{T,h}\|_2 \quad \le \quad C\,h\,M\Big(\frac{1}{\alpha}\Big)\,T\,(1+T)\,. \tag{16}$$

**Proof** Let us recall the definition of $R_T$ given in Lemma 2.1,

$$\begin{aligned} R_T(x,t) = -H(x-t)\big(D(T,t_0) + D(x_0,0)\big) + \frac{1}{M(\frac{1}{\alpha})}\,D(x_0,0)\,D(T,t_0) \\ +x\,D(T,t_0) + (1-t)\,D(x_0,0)\,, \quad \text{for some } x_0,\,t_0 \in [0,T[. \end{aligned}$$

For $x_0$, $t_0 \in [0,T[$, we have the estimates

$$|D(x_0,0)| \le M\Big(\frac{1}{\alpha}\Big)\,T \quad \text{and} \quad |D(T,t_0)| \le M\Big(\frac{1}{\alpha}\Big)\,T\,.$$

Consequently, for any $x,t \in [0,1]$

$$\big|R_T(x,t)\big| \quad \le \quad 4T\,M\Big(\frac{1}{\alpha}\Big)\,\Big(1+T\Big).$$

From $\int_\Omega b_i^h(x)\,dx = h$, and $\|B_{T,h}\|_2 \le \|B_{T,h}\|_F = \Big(\sum\limits_{1\le i,j\le n}\big(B_{T,h}\big)_{i,j}^2\Big)^{1/2}$ we deduce

$$\|B_{T,h}\|_2 \quad \le \quad h^2\,M\Big(\frac{1}{\alpha}\Big)\,4T\,\Big(\sum_{1\le i,j\le n}(1+T)^2\Big)^{1/2},$$

which concludes the proof. ■

# 4 Numerical Tests

In this section, we perform numerical tests for different positive, periodic and non-periodic coefficients $\alpha$. The step size $H$ is chosen proportional to $h$. In Section 4.1, we consider the case of $T$-periodic coefficients $\alpha$, with $T$ proportional to $h$, while Section 4.2 is devoted to non-periodic coefficients $\alpha$. In both cases, we compute the norm $\|\!|\tilde{R}_{H\leftarrow h}\,L_h^{-1}\tilde{P}_{h\leftarrow H} - A_H^{-1}|\!\|$ for different values of the grid parameters $h$, $H$, where the

operator $A$ is defined by $A = \frac{d}{dx}\Big(a\frac{d}{dx}\Big)$ and the coefficient $a$ is the piecewise harmonic average of $\alpha$ on the grid $\mathcal{T}_H$ given by formula (8), *i.e.* $a = \frac{1}{\theta(j)}$ for $0 \le j \le m$,

$$\theta(j) = \frac{1}{H}\int_{x_j^H}^{x_{j+1}^H} \frac{ds}{\alpha(s)}\,.$$

Particularly, $A = L_0$ for $\alpha$ periodic. In the figures of this section we denote the norm by

$$e(H,h) := \|\tilde{R}_{H\leftarrow h}\, L_h^{-1}\tilde{P}_{h\leftarrow H} - A_H^{-1}\|\,.$$

## 4.1 $T$-periodic coefficients

In order to compare our method with already existing homogenisation methods, we first consider a $T$-periodic coefficient $\alpha$. For each test we can choose three different parameters $h$, $H$, $T$. To each pair $(H,h)$ corresponds one numeric value $a$. This value allows us to compute the operator $A$. If the period $T$ is smaller than the step size $H$, and $H$ and $T$ are proportional,

$$\theta(j) = \frac{1}{H}\int_{x_j^H}^{x_{j+1}^H} \frac{ds}{\alpha(s)} = \frac{1}{T}\int_0^T \frac{ds}{\alpha(s)}\,,$$

which implies that the value $a$ is exactly the homogenised coefficient $\alpha_0$ given by the homogenisation theory (see (7)) and $A = L_0$. So in this case, the estimate (12) holds:

$$\|\tilde{R}_{H\leftarrow h}\, L_h^{-1}\tilde{P}_{h\leftarrow H} - A_H^{-1}\| \le C\left(\varepsilon(h) + T\,M\big(\frac{1}{\alpha}\big)\,(1+T) + \varepsilon_0(H)\right).$$

Currently we are dealing with $P^1$-FE approximation, if the operator $L_0$ is smooth enough, we can expect to get $\varepsilon_0(H) = \mathcal{O}(H^2)$ for $H \gg T$.
In the following test cases, for each value of $T$ three situations can occur: $H \gg T$, $H \approx T$, and $H \ll T$. In paragraph 4.1.1, the coefficient $\alpha$ is a smooth function of $T$, in paragraph 4.1.2, the coefficient $\alpha$ is continuous but not smooth, whereas in paragraph 4.1.3, $\alpha$ is piecewise constant. Let us note that for the following examples the numerical inverse Taylor expansion of $\mathcal{L}_{H,h}$ gives the coefficients $\beta_i$ of (6) such that

$$\beta_i \approx 0,\ \text{if } i \ne 2, \quad \beta_2 \approx \alpha_0 \quad \text{for } H > T\,,$$

which means that numerically the choice $A$ is appropriate.

### 4.1.1 Smooth coefficient, small amplitude

We consider the $T$-periodic positive coefficient $\alpha$ given by

$$\alpha(x+jT) = 3\,(\cos(5\,\frac{x}{T}))^3 + 30\,,\ x \in [0,T[\,,\ j \in \mathbb{Z}\,.$$

We compute the norm $\|\tilde{R}_{H\leftarrow h}\, L_h^{-1}\tilde{P}_{h\leftarrow H} - A_H^{-1}\|$ for $h = 1/4000$ and different coarse mesh sizes $H$ from $2000h = 1/2$ to $h$, and different periods $T \in \{1/25, 1/50, 1/100, 1/200\}$. The results are reported in Table 1. The convergence of $\|\tilde{R}_{H\leftarrow h}\, L_h^{-1}\tilde{P}_{h\leftarrow H} - A_H^{-1}\|$ can be observed on Figure 1. Globally the convergence rate of the norm $\|\tilde{R}_{H\leftarrow h}\, L_h^{-1}\tilde{P}_{h\leftarrow H} - A_H^{-1}\|$ is of order 1.5 with a jump around $H = T/2$. Let us remark that the value $H = T/2$ corresponds to the passage of the state $H \gg T$ to the state $H \ll T$ for which the coefficient $a$ is not any more the homogenised coefficient $\alpha_0$. For $H \gg T$, the results are consistent with estimate (12). Since we use $P^1$-elements, we have $\varepsilon_0(H) = \mathcal{O}(H^2)$. Moreover $h$ is small compared to $H$ and $T$, so that $\varepsilon(h)$ can be neglected. The term $T\,M(\frac{1}{\alpha})\,(1+T)$ behaves like $T\,M(\frac{1}{\alpha})$. When $H$ approaches $T$ the term $T\,M(\frac{1}{\alpha})\,(1+T)$ is gaining in importance compared to $\varepsilon_0(H)$.

| $H$ \ $T$ | $1/25$ $= 160h$ | $1/50$ $= 80h$ | $1/100$ $= 40h$ | $1/200$ $= 20h$ |
|---|---|---|---|---|
| $1/2 = 2000h$ | 2.99e-4 | 2.99e-4 | 2.99e-4 | 2.99e-4 |
| $1/5 = 800h$ | 7.93e-5 | 7.89e-5 | 7.88e-5 | 7.88e-5 |
| $1/10 = 400h$ | 2.55e-5 | 2.43e-5 | 2.38e-5 | 2.35e-5 |
| $1/20 = 200h$ | 9.32e-6 | 7.87e-6 | 7.13e-6 | 6.76e-6 |
| $1/25 = 160h$ | 7.23e-6 | 5.71e-6 | 4.96e-6 | 4.58e-6 |
| $1/50 = 80h$ | 1.13e-6 | 2.76e-6 | 1.95e-6 | 1.55e-6 |
| $1/100 = 40h$ | 7.28e-7 | 2.98e-7 | 1.18e-6 | 7.61e-7 |
| $1/200 = 20h$ | 2.58e-7 | 3.07e-7 | 8.93e-8 | 5.62e-7 |
| $1/250 = 16h$ | 1.70e-7 | 2.60e-7 | 3.66e-7 | 4.46e-7 |
| $1/400 = 10h$ | 6.81e-8 | 1.14e-7 | 1.37e-7 | 3.95e-8 |
| $1/500 = 8h$ | 4.37e-8 | 7.41e-8 | 1.22e-7 | 1.87e-7 |
| $1/1000 = 4h$ | 1.05e-8 | 1.82e-8 | 3.32e-8 | 5.48e-8 |
| $1/2000 = 2h$ | 2.12e-9 | 3.68e-9 | 6.75e-9 | 1.29e-8 |

Table 1: $\|\tilde{R}_{H\leftarrow h}\, L_h^{-1} \tilde{P}_{h\leftarrow H} - A_H^{-1}\|$, $h = 1/4000$, $\alpha(x) = 3\,(\cos(5\,\frac{x}{T}))^3 + 30$, $x \in [0, T[$.

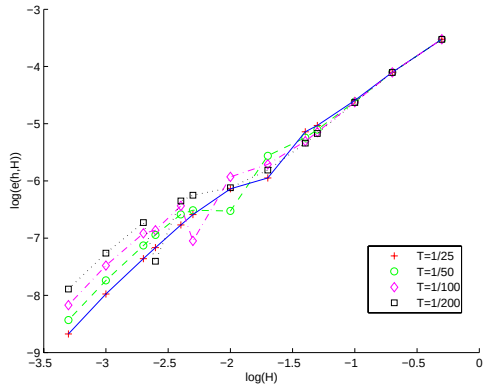


Figure 1: $\log\Big(\|\tilde{R}_{H\leftarrow h}\, L_h^{-1} \tilde{P}_{h\leftarrow H} - A_H^{-1}\|\Big)$ is represented as a function of $\log(H)$ for $h = 1/4000$ and $T \in \{1/25, 1/50, 1/100, 1/200\}$, $\alpha(x) = 3\,(\cos(5\,\frac{x}{T}))^3 + 30$, $x \in [0, T[$.

### 4.1.2 Non-smooth coefficient

We consider the following positive coefficient $\alpha$ (a 1D adaptation of a 2D coefficient from [12]):

$$\alpha(x) = \Big[1 + |\sin\frac{2\,\pi\,x}{T}|\Big]^{-1}, \quad \text{for } x \in [0,1]\,.$$

This coefficient is $\frac{T}{2}$-periodic, continuous but non-smooth at points $\frac{k\,\pi}{2}$, $k \in \mathbb{Z}$. We compute the norm $\|\tilde{R}_{H\leftarrow h}\, L_h^{-1} \tilde{P}_{h\leftarrow H} - A_H^{-1}\|$ for $h = 2^{-14}$ and different coarse mesh sizes $H = 2^{-k}$, $k \in [\![2, 11]\!]$, and different periods $T = 2^{-k}$, $k \in [\![1, 9]\!]$. The results are reported in Table 2. Globally the norm $\|\tilde{R}_{H\leftarrow h}\, L_h^{-1} \tilde{P}_{h\leftarrow H} - A_H^{-1}\|$ is decreasing toward 0 when $H$ is decreasing from $1/4$ to $2^3\,h$. Figure 2 shows the convergence of $\|\tilde{R}_{H\leftarrow h}\, L_h^{-1} \tilde{P}_{h\leftarrow H} - A_H^{-1}\|$ which is globally of order 2 with a jump around the value $H = T/8$. As in the previous example, the jump of the error $e(H,h) := \|\tilde{R}_{H\leftarrow h}\, L_h^{-1} \tilde{P}_{h\leftarrow H} - A_H^{-1}\|$ around the value $H = T/8$ corresponds to the jump of the coefficient $a$ from the homogenised one $\alpha_0$ (7) to its generalisation (8). Even though the coefficient $\alpha$ is not anymore smooth, we get a good convergence of the error between the discrete operators $\tilde{R}_{H\leftarrow h}\, L_h^{-1} \tilde{P}_{h\leftarrow H}$ and $A_H^{-1}$. Notice that for a fixed $H$, when $T \to 0$, $T \ll H$, the values $\|\tilde{R}_{H\leftarrow h}\, L_h^{-1} \tilde{P}_{h\leftarrow H} - A_H^{-1}\|$ are converging towards a certain limit noted $l_H$ (for example $l_{1/4} = 5.48 \times 10^{-3}$, $l_{1/8} = 1.69 \times 10^{-3}$, $l_{1/16} = 4.73 \times 10^{-4}$, $l_{1/32} = 1.29 \times 10^{-4}$, $l_{1/64} = 3.75 \times 10^{-5}$). Note that $l_H$ behaves almost in $\mathcal{O}(H^2)$.

| $H$ \ $T$ | $1/8$ $= 2^{11}\,h$ | $1/16$ $= 2^{10}\,h$ | $1/32$ $= 2^{9}\,h$ | $1/64$ $= 2^{8}\,h$ | $1/128$ $= 2^{7}\,h$ | $1/256$ $= 2^{6}\,h$ | $1/512$ $= 2^{5}\,h$ |
|---|---|---|---|---|---|---|---|
| 1/ 4 | 5.48e-3 | 5.48e-3 | 5.48e-3 | 5.48e-3 | 5.48e-3 | 5.48e-3 | 5.48e-3 |
| 1/ 8 | 1.69e-3 | 1.69e-3 | 1.69e-3 | 1.69e-3 | 1.69e-3 | 1.69e-3 | 1.69e-3 |
| 1/ 16 | 4.73e-4 | 4.73e-4 | 4.73e-4 | 4.73e-4 | 4.73e-4 | 4.73e-4 | 4.72e-4 |
| 1/ 32 | 1.98e-4 | 1.29e-4 | 1.29e-4 | 1.29e-4 | 1.29e-4 | 1.29e-4 | 1.29e-4 |
| 1/ 64 | 2.26e-4 | 5.12e-5 | 3.75e-5 | 3.75e-5 | 3.75e-5 | 3.75e-5 | 3.75e-5 |
| 1/ 128 | 6.14e-5 | 1.11e-4 | 1.36e-5 | 1.37e-5 | 1.36e-5 | 1.36e-5 | 1.36e-5 |
| 1/ 256 | 1.59e-5 | 2.96e-5 | 5.53e-5 | 4.06e-6 | 7.60e-6 | 7.59e-6 | 7.58e-6 |
| 1/ 512 | 4.04e-6 | 7.60e-6 | 1.45e-5 | 2.77e-5 | 1.79e-6 | 6.08e-6 | 6.07e-6 |
| 1/ 1024 | 1.02e-6 | 1.92e-6 | 3.70e-6 | 7.19e-6 | 1.38e-5 | 1.33e-6 | 5.65e-6 |
| 1/ 2048 | 2.52e-7 | 4.79e-7 | 9.27e-7 | 1.81e-6 | 2.52e-6 | 2.58e-6 | 1.21e-6 |

Table 2: $\|\tilde{R}_{H\leftarrow h}\, L_h^{-1} \tilde{P}_{h\leftarrow H} - A_H^{-1}\|$, for different values of $h = 2^{-14}$, $\alpha(x) = \Big[1 + |\sin\frac{2\,\pi\,x}{T}|\Big]^{-1}$, $a \approx 0.611$ for $H \gg T$.

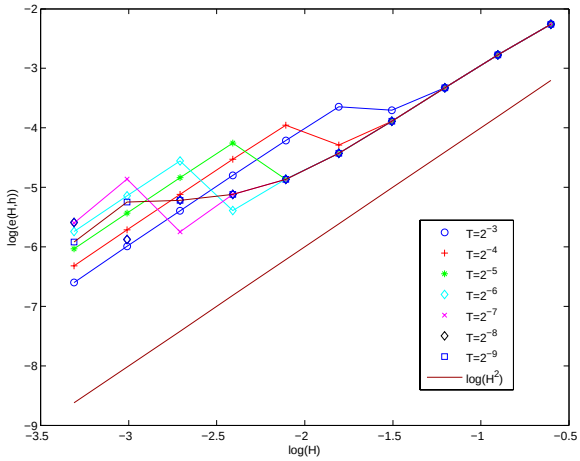


Figure 2: $\log\left(\left\|\left\|\tilde{R}_{H\leftarrow h}\, L_h^{-1}\tilde{P}_{h\leftarrow H} - A_H^{-1}\right\|\right\|\right)$ is represented as a function of $\log(H)$ for $h = 2^{-14}$ and $T = 2^{-k}$, $k \in [1, 9]$, $\alpha(x) = \left[1 + |\sin\frac{2\,\pi\,x}{T}|\right]^{-1}$.

### 4.1.3 Piecewise constant coefficient

We consider the $T$-periodic, piecewise constant coefficient $\alpha > 0$, defined on a period $[0, T[$ by:

$$\alpha(x) = \begin{cases} 8.1\,, & x \in [0, \frac{T}{4}[ \\ 0.3\,, & x \in [\frac{T}{4}, \frac{T}{2}[ \\ 20.55\,, & x \in [\frac{T}{2}, \frac{3\,T}{4}[ \\ 1.0\,, & x \in [\frac{3\,T}{4}, T[\,. \end{cases} \tag{17}$$

We compute the norm $\left\|\left\|\tilde{R}_{H\leftarrow h}\, L_h^{-1}\tilde{P}_{h\leftarrow H} - A_H^{-1}\right\|\right\|$ for different values of $h$ and $H$. Let us consider the following situations:

1. $h = 2.5 \times 10^{-4}$, $H$ takes its values between $1/2$ and $h$, and the period $T$ is varying between $T = 1/25$ and $T = 1/200$.
2. $h = 10^{-5}$, $H$ takes its values between $1/2$ and $50\,h$, and the period $T$ is varying between $T = 10^{-3}$ and $T = 10^{-4}$.

The results of the computation of the norm $\left\|\left\|\tilde{R}_{H\leftarrow h}\, L_h^{-1}\tilde{P}_{h\leftarrow H} - A_H^{-1}\right\|\right\|$ are reported on the left side of Table 3 for $h = 10^{-4}$ and on the right side for $h = 10^{-5}$. Figure 3 shows the logarithm of the norm as a function of $\log(H)$ for $h = 10^{-5}$ and different values of $T$.
In both cases, the grid parameter $h$ (in comparison with $H$ and $T$) is small enough and has a weak influence on the variation of the norm (we can observe in Table 3 that this is true at least for large values of $H$). Let us mention that for the value $h = 10^{-5}$, for a fixed value of $T$ the convergence rate is behaving as a function of $H$. For example for $T = 1/5000$, the convergence is almost of order 2, when $H$ is very large and decreases towards 1.5 until $H = 1/100$ and then the convergence almost stops. When $H$ is large compared to $T$, the influence of $\varepsilon_0(H)$ is greater than the influence of the period. At some point, when $H$ becomes small enough, the term depending on $T$ in the right-hand side of estimate (12) becomes comparable with $\varepsilon_0(H)$, which does not have such a large effect any more. Moreover for a fixed $H$, when $T \to 0$, $T \ll H$, the value of the norm is converging and decreasing towards a certain limit noted $l_H$ (for example $l_{1/2} = 9.96 \times 10^{-3}$, $l_{1/5} = 2.62 \times 10^{-3}$, $l_{1/10} = 7.75 \times 10^{-4}$, $l_{1/20} = 2.13 \times 10^{-4}$, $l_{1/25} = 1.39 \times 10^{-4}$). This is the result expected from the homogenisation theory. We consider now the solution of problem (2) for a constant right-hand side $f = 10$ and the coefficient $\alpha$ defined in (17) with a period $T = 2^{-3}$. Figure 4 depicts the discrete solution $u_h = L_h^{-1} f$, the homogenised solution $u_0 = L_0^{-1} f$, and the discrete solution given by $u_{H,h} = \mathcal{L}_{H,h}^{-1} f$ for the step sizes $h = 2^{-13}$ and $H = 2^{-7}$. The solid-line plots the discrete $P^1$-solution $u_h$ on $\mathcal{T}_h$, whereas the dot-line

| $H$ \ $T$ | $1/25$ $= 160h$ | $1/50$ $= 80h$ | $1/100$ $= 40h$ | $1/200$ $= 20h$ |
|---|---|---|---|---|
| $1/2 = 2000h$ | 9.96e-3 | 9.96e-3 | 9.96e-3 | 9.96e-3 |
| $1/5 = 800h$ | 2.68e-3 | 2.64e-3 | 2.63e-3 | 2.62e-3 |
| $1/10 = 400h$ | 9.44e-4 | 8.50e-4 | 8.05e-4 | 7.82e-4 |
| $1/20 = 200h$ | 4.77e-4 | 3.15e-4 | 2.61e-4 | 2.36e-4 |
| $1/25 = 160h$ | 3.48e-4 | 2.42e-4 | 1.89e-4 | 1.64e-4 |
| $1/50 = 80h$ | 1.46e-3 | 1.47e-4 | 9.16e-5 | 6.37e-5 |
| $1/100 = 40h$ | 1.80e-5 | 7.35e-4 | 6.66e-5 | 3.79e-5 |
| $1/200 = 20h$ | 6.15e-6 | 4.52e-6 | 3.71e-4 | 3.14e-5 |
| $1/400 = 10h$ | 1.66e-6 | 1.53e-6 | 1.13e-6 | 1.86e-4 |
| $1/500 = 8h$ | 1.07e-6 | 7.50e-5 | 1.39e-4 | 1.32e-4 |
| $1/1000 = 4h$ | 2.58e-7 | 2.54e-7 | 3.82e-5 | 6.98e-5 |
| $1/2000 = 2h$ | 5.18e-8 | 5.16e-8 | 5.07e-8 | 1.71e-5 |

| $H$ \ $T$ | $1/500$ $= 200h$ | $1/1000$ $= 100h$ | $1/2500$ $= 40h$ | $1/5000$ $= 20h$ |
|---|---|---|---|---|
| $1/2 = 50000h$ | 9.96e-3 | 9.96e-3 | 9.96e-3 | 9.96e-3 |
| $1/5 = 20000h$ | 2.62e-3 | 2.62e-3 | 2.62e-3 | 2.62e-3 |
| $1/10 = 10000h$ | 7.75e-4 | 7.75e-4 | 7.75e-4 | 7.75e-4 |
| $1/20 = 5000h$ | 2.21e-4 | 2.16e-4 | 2.13e-4 | 2.13e-4 |
| $1/25 = 4000h$ | 1.48e-4 | 1.43e-4 | 1.39e-4 | 1.39e-4 |
| $1/50 = 2000h$ | 4.70e-5 | 4.15e-5 | 3.81e-5 | 3.69e-5 |
| $1/100 = 1000h$ | 2.06e-5 | 1.49e-5 | 1.15e-5 | 1.03e-5 |
| $1/200 = 500h$ | 1.43e-5 | 8.14e-6 | 4.65e-6 | 3.48e-6 |
| $1/250 = 400h$ | 1.32e-5 | 7.33e-6 | 3.82e-6 | 2.65e-6 |
| $1/500 = 200h$ | 1.21e-5 | 6.24e-6 | 2.72e-6 | 1.54e-6 |
| $1/1000 = 100h$ | – | 5.94e-6 | 2.50e-6 | 1.27e-6 |
| $1/2000 = 50h$ | – | – | 2.46e-6 | 1.21e-6 |

Table 3: $\|\!|\tilde{R}_{H\leftarrow h}\, L_h^{-1} \tilde{P}_{h\leftarrow H} - A_H^{-1}|\!\|$, $\alpha$ piecewise const, $a \simeq 0.887813$ if $H \geq T$. Left: $h = 2.5 \times 10^{-4}$. Right: $h = 10^{-5}$.

with squares represents the homogenised solution $u_0$. The dots display the values of $u_{H,h}$ on the grid $\mathcal{T}_H$. The values of $u_{H,h}$ are matching the discrete solution $u_h$. The discrete solution $u_{H,h}$ captures well the details of $u_h$, while the classical homogenised solution $u_0$ interpolates the fine solution $u_h$.

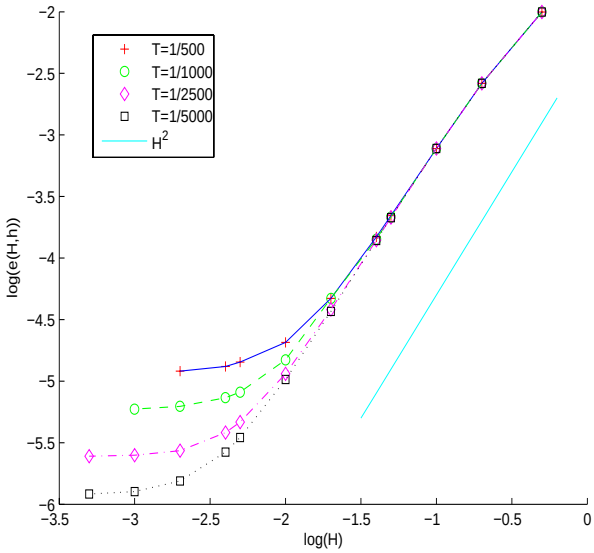


Figure 3: $\log\Big(\|\!|\tilde{R}_{H\leftarrow h}\, L_h^{-1} \tilde{P}_{h\leftarrow H} - A_H^{-1}|\!\|\Big)$ is represented for $\alpha(\cdot)$ defined by (17), as a function of $\log(H)$ for $h = 10^{-5}$ and $T = 1/500,\ 1/1000,\ 1/2500,\ 1/5000$.

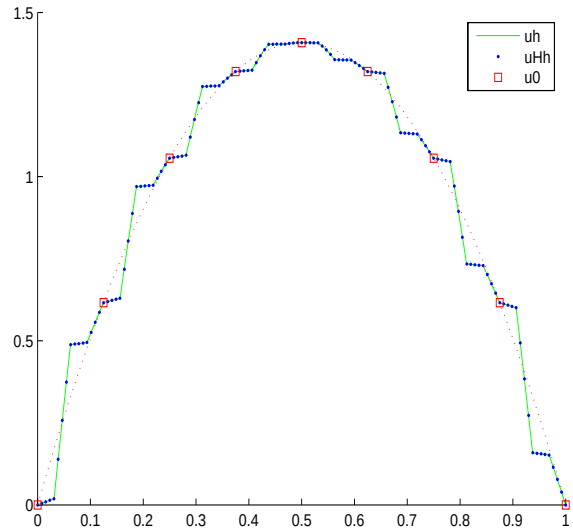


Figure 4: Representation of $u_h = L_h^{-1} f$, $u_0 = L_0^{-1} f$, $u_{H,h} = \mathcal{L}_{H,h}^{-1} f$, for $\alpha(\cdot)$ defined by (17). $h = 2^{-13}$, $T = 2^{-3}$, and $H = 2^{-7}$.

## 4.2 Non-periodic coefficient

Regarding the previous numerical experiments, it seems that the discrete operator $\mathcal{L}_{H,h} = \big(\tilde{R}_{H\leftarrow h} L_h^{-1} \tilde{P}_{h\leftarrow H}\big)^{-1}$ is behaving as the discretisation of an elliptic operator, namely $L_0$, in the case of periodic coefficients. Therefore, we are now considering non-periodic, positive coefficients $\alpha$ defined on $\Omega$. The coefficient $\alpha_0$ is computed on each segment $[x_j^H, x_{j+1}^H]$ by formula (8). In the following, we propose three different test cases and for each of them compute the norm $\|\!|\tilde{R}_{H\leftarrow h}\, L_h^{-1} \tilde{P}_{h\leftarrow H} - A_H^{-1}|\!\|$.

### 4.2.1 Smooth coefficients

Let us consider the following non-periodic coefficient $\alpha$ given by $\alpha(x) = 2 + \sin(27\, x^2)$ on $\Omega$. This coefficient is a smooth function. The computed values of the norm $\|\!|\tilde{R}_{H\leftarrow h}\, L_h^{-1} \tilde{P}_{h\leftarrow H} - A_H^{-1}|\!\|$ for $h \in \{1/1000,\ 1/2000,$

1/4000, 1/8000} and values of $H$ between 1/2 and $h$ are given in Table 4. The dependence of the norm on $H$, for $h = 1/8000$, is shown on Figure 5. The results do not depend on the choice of the step size $h$. For $H$ fixed, $H > 1/500$, the values of the norm $\|\tilde{R}_{H\leftarrow h}\, L_h^{-1} \tilde{P}_{h\leftarrow H} - A_H^{-1}\|$ related to different $h$ are almost the same. Moreover the convergence of the norm is almost of order 2 for $H < 1/25$, *i.e.* the method is efficient for coarse meshes.

| $H$ \ $h$ | 1/ 1000 | 1/ 2000 | 1/ 4000 | 1/ 8000 |
|---|---|---|---|---|
| 1/ 2 | 3.01e-3 | 3.00e-3 | 3.00e-3 | 3.00e-3 |
| 1/ 5 | 1.88e-3 | 1.88e-3 | 1.88e-3 | 1.88e-3 |
| 1/ 10 | 1.05e-3 | 1.06e-3 | 1.06e-3 | 1.06e-3 |
| 1/ 20 | 4.64e-4 | 4.63e-4 | 4.63e-4 | 4.62e-4 |
| 1/ 25 | 3.12e-4 | 3.13e-4 | 3.13e-4 | 3.14e-4 |
| 1/ 50 | 9.99e-5 | 1.00e-4 | 1.00e-4 | 1.00e-4 |
| 1/ 100 | 2.69e-5 | 2.71e-5 | 2.71e-5 | 2.71e-5 |
| 1/ 200 | 6.69e-6 | 6.90e-6 | 6.95e-6 | 6.96e-6 |
| 1/ 250 | 4.20e-6 | 4.41e-6 | 4.46e-6 | 4.47e-6 |
| 1/ 400 | – | 1.69e-6 | 1.74e-6 | 1.75e-6 |
| 1/ 500 | 8.46e-7 | 1.06e-6 | 1.11e-6 | 1.12e-6 |
| 1/ 1000 | 1.32e-14 | 2.12e-7 | 2.65e-7 | 2.78e-7 |
| 1/ 2000 | – | 2.41e-14 | 5.31e-8 | 6.63e-8 |
| 1/ 4000 | – | – | 6.96e-14 | 1.33e-8 |

Table 4: $\|\tilde{R}_{H\leftarrow h}\, L_h^{-1} \tilde{P}_{h\leftarrow H} - A_H^{-1}\|$, for different values of $h = 1/1000,\ 1/2000,\ 1/4000,\ 1/8000$, $\alpha(x) = 2 + \sin(27\,x^2)$.

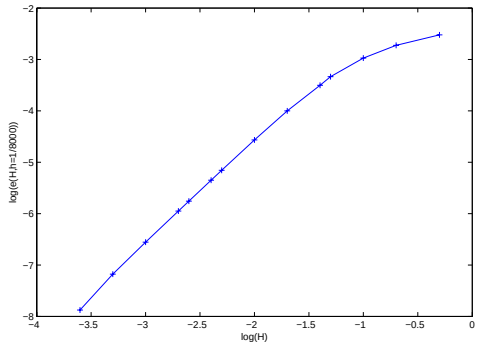


Figure 5: $\log\Big(\|\tilde{R}_{H\leftarrow h}\, L_h^{-1} \tilde{P}_{h\leftarrow H} - A_H^{-1}\|\Big)$ is represented as a function of $\log(H)$ for $h = 1/8000$ where $\alpha(x) = 2 + \sin(27\,x^2)$.

### 4.2.2 Piecewise constant coefficients

We consider the coefficient $\alpha(x) = 1 + |(1-x)\,\lceil \sin(500\,x)\,\cos(300\,x)\,\exp(5\,x)\rceil|$ defined on $\Omega$, where $\lceil x\rceil = \max\{i \in \mathbb{Z} : i - 1 < x\}$. The coefficient $\alpha$ is piecewise constant, its value is oscillating between 1 and 12. We compute the norm $\|\tilde{R}_{H\leftarrow h}\, L_h^{-1} \tilde{P}_{h\leftarrow H} - A_H^{-1}\|$ for $h$ equal to 1/1000, 1/2000, 1/4000, or 1/8000. For each $h$ we investigate different values of $H$ between 1/2 and $h$. The results are assembled in Table 5. The dependence of the norm on $H$, for $h = 1/8000$, is shown on Figure 6. The norm is practically independent of the value of $h$ (for $H > 1/500$, the influence of $h$ is very small). The coefficient $\alpha$ is not any more a smooth function, nevertheless, the convergence rate of the norm $\|\tilde{R}_{H\leftarrow h}\, L_h^{-1} \tilde{P}_{h\leftarrow H} - A_H^{-1}\|$ is still good. When $H$ is converging toward $h$, the norm $\|\tilde{R}_{H\leftarrow h}\, L_h^{-1} \tilde{P}_{h\leftarrow H} - A_H^{-1}\|$ converges toward 0 with global order 1. The convergence is accelerating when $H < 1/400$.

| $H$ \ $h$ | 1/ 1000 | 1/ 2000 | 1/ 4000 | 1/ 8000 |
|---|---|---|---|---|
| 1/ 5 | 1.78e-3 | 1.78e-3 | 1.77e-3 | 1.78e-3 |
| 1/ 10 | 7.53e-4 | 7.87e-4 | 7.80e-4 | 7.84e-4 |
| 1/ 20 | 3.53e-4 | 3.71e-4 | 3.72e-4 | 3.71e-4 |
| 1/ 25 | 2.47e-4 | 2.39e-4 | 2.38e-4 | 2.38e-4 |
| 1/ 50 | 1.13e-4 | 1.07e-4 | 1.06e-4 | 1.07e-4 |
| 1/ 100 | 8.93e-5 | 8.67e-5 | 8.79e-5 | 8.76e-5 |
| 1/ 200 | 5.46e-5 | 5.12e-5 | 5.03e-5 | 4.96e-5 |
| 1/ 250 | 4.60e-5 | 4.35e-5 | 4.42e-5 | 4.43e-5 |
| 1/ 400 | – | 2.75e-5 | 2.77e-5 | 2.75e-5 |
| 1/ 500 | 2.04e-5 | 2.07e-5 | 2.07e-5 | 2.07e-5 |
| 1/ 1000 | 2.16e-14 | 7.45e-6 | 7.81e-6 | 7.85e-6 |
| 1/ 2000 | – | 1.22e-13 | 2.43e-6 | 2.64e-6 |
| 1/ 4000 | – | – | 3.14e-13 | 7.84e-7 |

Table 5: $\|\tilde{R}_{H\leftarrow h}\, L_h^{-1} \tilde{P}_{h\leftarrow H} - A_H^{-1}\|$, for different values of $h = 1/1000,\ 1/2000,\ 1/4000,\ 1/8000$, $\alpha(x) = 1 + |(1-x)\,\lceil \sin(500\,x)\,\cos(300\,x)\,\exp(5\,x)\rceil|$.

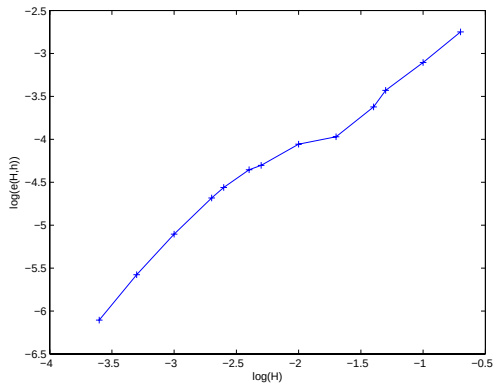


Figure 6: $\log\Big(\|\tilde{R}_{H\leftarrow h}\, L_h^{-1} \tilde{P}_{h\leftarrow H} - A_H^{-1}\|\Big)$ is represented as a function of $\log(H)$ for $h = 1/8000$ where $\alpha(x) = 1 + |(1-x)\,\lceil \sin(500\,x)\,\cos(300\,x)\,\exp(5\,x)\rceil|$.

### 4.2.3 Oscillatory coefficients

Let us consider the non-periodic coefficient $\alpha$ given by $\alpha(x) = \left[2 - \sin(2\,\pi \tan(\frac{x\,\pi}{2}))\right]^{-1}$ on $\Omega$. This function contains a continuum of scales (cf. [7]). The norms $\|\tilde{R}_{H\leftarrow h}\, L_h^{-1} \tilde{P}_{h\leftarrow H} - A_H^{-1}\|$ for the values of $h \in \{1/1000, 1/2000, 1/4000, 1/8000\}$ and values of $H$ between $1/2$ and $h$ are given in Table 6. We can observe that the dependence of $\|\tilde{R}_{H\leftarrow h}\, L_h^{-1} \tilde{P}_{h\leftarrow H} - A_H^{-1}\|$ on $h$ is small. Notwithstanding the very oscillatory behaviour of the coefficient $\alpha$, the convergence of the norm is good (globally order 1). The dependence of the norm on $H$, for $h = 1/8000$, is shown on Figure 7.

| $H$ \ $h$ | 1/ 1000 | 1/ 2000 | 1/ 4000 | 1/ 8000 |
|---|---|---|---|---|
| 1/2 | 8.60e-3 | 8.58e-3 | 8.59e-3 | 8.61e-3 |
| 1/5 | 7.70e-3 | 7.68e-3 | 7.68e-3 | 7.68e-3 |
| 1/10 | 3.36e-3 | 3.35e-3 | 3.35e-3 | 3.34e-3 |
| 1/20 | 1.08e-3 | 1.06e-3 | 1.04e-3 | 1.04e-3 |
| 1/25 | 8.56e-4 | 8.57e-4 | 8.59e-4 | 8.61e-4 |
| 1/50 | 3.22e-4 | 3.22e-4 | 3.22e-4 | 3.23e-4 |
| 1/100 | 1.94e-4 | 1.91e-4 | 1.89e-4 | 1.88e-4 |
| 1/200 | 9.23e-5 | 8.29e-5 | 7.90e-5 | 7.80e-5 |
| 1/250 | 7.07e-5 | 6.21e-5 | 5.89e-5 | 5.77e-5 |
| 1/400 | – | 3.84e-5 | 3.57e-5 | 3.46e-5 |
| 1/500 | 3.42e-5 | 2.97e-5 | 2.65e-5 | 2.54e-5 |
| 1/1000 | 2.82e-15 | 1.30e-5 | 1.37e-5 | 1.02e-5 |
| 1/2000 | – | 4.55e-14 | 5.63e-6 | 5.58e-6 |
| 1/4000 | – | – | 6.53e-14 | 2.49e-6 |

Table 6: $\|\tilde{R}_{H\leftarrow h}\, L_h^{-1} \tilde{P}_{h\leftarrow H} - A_H^{-1}\|$, for $h = 1/1000,\ 1/2000,\ 1/4000,\ 1/8000$, $\alpha(x) = \left[2 - \sin(2\,\pi \tan(\frac{x\,\pi}{2}))\right]^{-1}$.

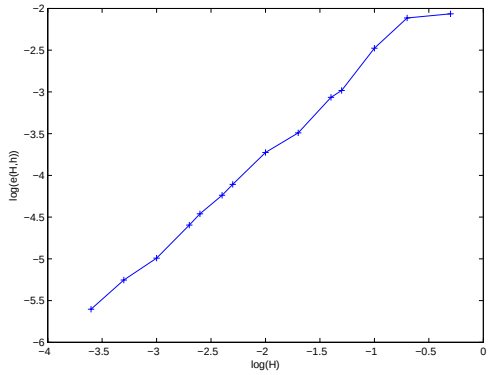


Figure 7: $\log\left(\|\tilde{R}_{H\leftarrow h}\, L_h^{-1} \tilde{P}_{h\leftarrow H} - A_H^{-1}\|\right)$ is represented as a function of $\log(H)$ for $h = 1/8000$ where $\alpha(x) = \left[2 - \sin(2\,\pi \tan(\frac{x\,\pi}{2}))\right]^{-1}$.

# 5 Conclusion

Theoretically and numerically, the discrete operator $\mathcal{L}_{H,h} := \left(\tilde{R}_{H\leftarrow h} L_h^{-1} \tilde{P}_{h\leftarrow H}\right)^{-1}$ on the coarse mesh behaves like the discretisation of an elliptic operator. One possible approximation is given by $A = -\frac{d}{dx}\left(a\,\frac{d}{dx}\right)$, where $a$ is the piecewise harmonic average of $\alpha$ defined by (8). It means that

$$A_H^{-1} \approx \tilde{R}_{H\leftarrow h} L_h^{-1} \tilde{P}_{h\leftarrow H}\,, \qquad \text{for } h \text{ small enough,}$$

holds also for jumping or non-smooth coefficients without any conditions of periodicity. Moreover, in the periodic case, for a step size $H$ larger than $T$ the operator $A$ is in fact exactly the homogenised operator $L_0$.

Thus, the discrete operator $\mathcal{L}_{H,h}$ is proved to be suitable in 1D: It behaves as a discretisation of the classical homogenisation operator for periodic coefficients; for non periodic and jumping coefficients the quality of the discretisation given by $\mathcal{L}_{H,h}$ is good.

The computation of this discrete operator $\mathcal{L}_{H,h}$ is available for any dimension. Nevertheless, the theoretical analyse might be difficult, since the Green function is not analytically available. However, the numerical experiments should be extended to higher dimension by computing directly $\mathcal{L}_{H,h} = \left(\tilde{R}_{H\leftarrow h} L_h^{-1} \tilde{P}_{h\leftarrow H}\right)^{-1}$.

# References


[1] T. Arbogast. Analysis of a two-scale, locally conservative subgrid upscaling for elliptic problems. *SIAM J. Numer. Anal.*, 42(2):576–598, 2004.

[2] I. Babuška and J. E. Osborn. Generalized finite element methods: their performance and their relation to mixed methods. *SIAM J. Numer. Anal.*, 20(3):510–536, 1983.

[3] M. Bebendorf and W. Hackbusch. Existence of $\mathcal{H}$-Matrix Approximants to the inverse FE-matrix of elliptic operators with $L^\infty$-coefficients. *Numer. Math.*, 95(1):1–28, 2003.

[4] A. Bensoussan, J-L. Lions, and G. Papanicolaou. *Asymptotic analysis for periodic structures*, volume 5 of *Studies in Mathematics and its Applications*. North-Holland Publishing Co., Amsterdam, 1978.

[5] M. E. Brewster and G. Beylkin. A multiresolution strategy for numerical homogenization. *Appl. Comput. Harmon. Anal.*, 2(4):327–349, 1995.

[6] F. Brezzi. Interacting with the subgrid world. In *Numerical analysis 1999 (Dundee)*, volume 420 of *Chapman & Hall/CRC Res. Notes Math.*, pages 69–82. Chapman & Hall/CRC, Boca Raton, FL, 2000.

[7] A. C. Gilbert. A comparison of multiresolution and classical one-dimensional homogenization schemes. *Appl. Comput. Harmon. Anal.*, 5(1):1–35, 1998.

[8] L. Grasedyck and W. Hackbusch. Construction and arithmetics of $\mathcal{H}$-Matrices. *Computing*, 70:295–334, 2003.

[9] W. Hackbusch. *Multigrid methods and applications*, volume 4 of *Springer Series in Computational Mathematics*. Springer-Verlag, Berlin, 2nd edition, 1985.

[10] W. Hackbusch. Hierarchische Matrizen-Algorithmen und Analysis. Vorlesungsmanuskript 2005.

[11] T. Y. Hou and X.-H. Wu. A multiscale finite element method for elliptic problems in composite materials and porous media. *J. Comput. Phys.*, 134(1):169–189, 1997.

[12] T. Y. Hou, X-H. Wu, and Z. Cai. Convergence of a multiscale finite element method for elliptic problems with rapidly oscillating coefficients. *Math. Comp.*, 68(227):913–943, 1999.

[13] T. J. R. Hughes. Multiscale phenomena: Green's functions, the Dirichlet-to-Neumann formulation, subgrid scale models, bubbles and the origins of stabilized methods. *Comput. Methods Appl. Mech. Engrg.*, 127(1-4):387–401, 1995.

[14] T. J. R. Hughes, G. R. Feijóo, L. Mazzei, and J-B. Quincy. The variational multiscale method–a paradigm for computational mechanics. *Comput. Methods Appl. Mech. Engrg.*, 166(1-2):3–24, 1998.

[15] E. Weinan and B. Engquist. The heterogeous multiscale methods. *Comm. Math. Sci.*, 1(1):87–133, 2003.